멤브레인(Membrane Journal)
Vol.8, No.1, March, 1998, 11-21

총 설

유리고분자의 용매전달특성 및 그 해석

김 덕 준

성균관대학교 화학공학과
(1998년 1월 30일 접수)

Solvent Transport Characteristics of Glassy Polymers and its Analysis

Dukjoon Kim

Department of Chemical Engineering, Sung Kyun Kwan University Suwon, Kyunggi 440-746, Korea
(*Received January 31, 1998*)

1. Introduction

The study on penetrant transport in glassy polymers has been actively pursued for decades because of its growing significance in polymer processing and related applications such as not only membranes, but corrosion protective coatings, microlithography, microelectronic fabrication, etc. In membranes application of polymeric materials, successful utilization requires understanding of how solvents penetrate, swell, and sometimes dissolve polymeric materials under various environmental conditions, as their permselective performance is significantly affected by it. The expose of polymer membranes to solvents may result in the structural failure due to mechanical softening, embrittlement or crazing.

For general polymer-solvent systems, the transport behavior is affected by a variation of solvent temperature and concentration. Even Fick's law is the most frequently used expression to describe normal solvent transport behavior in general solid materials, it is not always useful to describe many anomalous behavior which are usually observed in many practical circumstances. In this contribution, the sovent transport phenomena in polymer systems experimentally observed were terminologically defined, the transport models founded on a few concrete theories were presented, and finally, the prediction of a variety of solvent transport behavior were represented for dodecane/polystyrene systems with a transport model.

2. Experimental Phenomenology

Penetrant transport in glassy polymers is characterized as Fickian, Case II, Super Case II and anomalous transport [1-6]. Fickian transport is characterized by a linear relationship between the initial weight gain and the square root of time with a smooth and continuous concentration profile throughout the sample. Case II transport was firstly defined by Alfrey *et al.* [7]. Several characteristic features of Case II transport include: (i) a sharp boundary separating an inner glassy core of zero penetrant concentration from an outer swollen rubber shell of uniform concentration; (ii) a front advancing at a constant velocity; and (iii) penetrant uptake proportional to time. Super Case II transport is characterized by a very distinct acceleration in sorption rate in the later stages of the uptake. Transport processes which fall between Fickian and Case II processes are termed anomalous transport.

Vrentas, Duda and other collaborators [8-10] defined the diffusion Deborah number, De, as a means of characterizing penetrant transport processes in polymer systems. This dimensionless group is the ratio of the diffusion time to the relaxation time of polymer chains during the transport process. If the diffusional and the relaxational resistances are the same order of magnitude, non-Fickian transport is observed.

A generalized expression for the transport kinetics is written as:

$$\frac{M_t}{M_\infty} = kt^n \tag{1}$$

where k is a constant incorporating characteristics of macromolecule and penetrant system and n is the diffusional exponent which is indication of the transport mechanism. The value of exponent n associated with the value of De is affected by the sample geometry [11].

3. Transport Models

When a penetrant diffuses into a polymer sample, the macromolecular chains rearrange toward new conformations where the rate of relaxation depends on the solvent concentration. The relative rates of penetrant diffusion and macromolecular chain relaxation to new conformations determine the nature of the transport process and lead to a wide variety of penetrant transportt phenomena such as Fickian and non-Fickian including Case II, Super Case II and anomalous. Particular aspects of these non-Fickian transport have been described by numerous models based on Fick's law, linear irreversible thermodynamics (LIT), and rational thermodynamics.

Fick's law describes the random motion of a diffusant molecule in an isotropic fluid or solid media. Diffusion models applying Fick's law are useful to describe the specific transport phenomena because of their relatively easy solution by analytical or numerical methods. The adjustable material properties are generally determined by fitting the experimental data to the model. A particular aspect of non-Fickian transport is often described by different models considering i) a convective term in the penetrant flux [12-14]; ii) changes in the polymer morphology resulting in a variable penetrant diffusion coefficient [15- 18]; and iii) non-Fickian propagation of a swelling front [14, 19-22]. Because a specific model cannot describe all transport phenomena, a more general model is needed to describe easily a wider range of transport phenomena.

Linear irreversible thermodynamics (LIT) suggests that the fluxes can be expressed in terms of linear combinations of all allowable forces, e.g. chemical potential gradient, temperature gradient, and stress distribution at non-equilibrium conditions near the equilibrium state. Some models applying the LIT theory [4-6, 23, 24] can predict anomalous transport with limited agreement with experiments. But since LIT is valid for only small perturbations away from equilibrium states, it may not be appropriate to describe mixtures which experience continuous macromolecular relaxation or inherently non-equilibrium character of glassy materials such as viscoelastic polymers.

Rational thermodynamics combines both mechanical and thermodynamic approachs without limitations on the departure from the equilibrium state. This framework satisfies the Clausius-Duhem entropy inequality as well as the conservation of mass, momentum and energy for each component. The entropy inequality places restrictions on the constitutive equations for all admissible thermodynamic processes [25, 26]. Application of this admissibility criteria to materials with memory [27-29] allows us to address viscoelastic behavior in penetrant/polymer mixtures. Transport models applying rational thermodynamics are particularly useful in describing viscoelastic behavior of glassy to rubbery transition during penetrant transport since their applicability encompasses both equilibrium and non-equilibrium characters.

4. A Model Developed Founded on Rational Thermodynamics

Continuum thermodynamics requires that the

entropy inequality be satisfied, stating that the rate of local entropy production is non-negative for all admissible processes. This requirement places the restrictions on the constitutive equations for a simple mixture under isothermal conditions in the absence of chemical reactions. Following is a brief description of a self- consistent transport model which has been recently developed and verified [30, 31].

The penetrant diffusive flux into polymers is enhanced by several driving forces such as temperature gradient, species' inertial and body forces acting on the components as well as chemical potential and stress gradients. For an isothermal, binary mixture under the condition of constant body forces and negligible inertial contribution, the new transport model is expressed as equation (2).

$$\boldsymbol{j}_1 = \frac{\rho_1 w_2^2 M_1 D_{12}}{RT}\left(\nabla \mu_1 + \frac{1}{\rho_2}\nabla \cdot \boldsymbol{T}_2\right) \tag{2}$$

Here, $\mathbf{j}_1$ is the mass flux of the penetrant, ρ_1 is the penetrant density, ω_2 is the polymer weight fraction, M_1 is the molecular weight of penetrant, D_{12} is the mutual diffusion coefficient, μ_1 is the penetrant chemical potential and $\mathbf{T}_2$ is the polymer stress.

The partial stress tensors and the solvent chemical potential were expressed as in equations (3) and (4).

$$\begin{aligned}\boldsymbol{T}_2 = {} & \phi_2 G_E\left[\boldsymbol{E} - \frac{\boldsymbol{E}:\boldsymbol{I}}{3}\boldsymbol{I}\right] + \frac{\phi_2 K_E}{2}\boldsymbol{E}:\boldsymbol{I} \\ & + \frac{\phi_2}{2}\boldsymbol{B}(t)\int_{-\infty}^{t} K_\Delta[\phi_2(t), t^* - \xi^*]\frac{dI(\xi)}{d\xi}\,d\xi \\ & + \phi_2\int_{-\infty}^{t} G_\Delta[\phi_2(t), t^* - \xi^*]\left[\boldsymbol{B}(t)\cdot \frac{d\,\boldsymbol{C}_{1}(\xi)}{d\xi}\boldsymbol{B}(t) - \frac{1}{3}\boldsymbol{B}(t)\frac{dI_{(}\xi)}{d\xi}\right]d\xi\end{aligned} \tag{3}$$

$$\mu_1 = \frac{RT}{M_1}\left[\ln\phi_1 + 1 - \phi_1 + \chi_1\,(1-\phi_1)^2\right] \tag{4}$$

Here, **B** is the left Cauchy-Green deformation tensor, **C** is the right Cauchy-Green deformation tensor and **E** = **B** - **I**. The terms, G_E and K_E are the elastic shear and bulk moduli. The material times, t* and ξ*, are defined by:

$$t^* = \int_0^t \frac{d\zeta}{a[\,T(\zeta), \phi_1]} \tag{5.a}$$

$$\xi^* = \int_0^\xi \frac{d\zeta}{a[\,T(\zeta), \phi_1]} \tag{5.b}$$

where a[T, $\rho\varphi_1$] is the generalization of the well known time temperature shift factor to consider the effect of solvent concentration on the relaxation processes.

The theoretical framework represented in equation (2) with equations (3), (4) and (5) may cover various types of mass transport phenomena in penetrant/polymer systems and address the interplay between penetrant diffusion and polymer mechanical relaxation.

5. Model Predicted Transport Behavior of Dodecane in Polystyrene

5.1. Description of Material Parameters

Application of the transport model requires that all material parameters (G, K, D, etc.) employed in equations from (2) to (5) be described in appropriate functional forms. Followings are the functional expressions for the material parameters measured for dodecane/polystyrene systems using various techniques.

The temperature dependence of specific volume of polystyrene and dodecane, V_1 and V_2, respectively, was determined from the PVT measurements [32].

$$V_1 = A_{11} + A_{12}T + A_{13}T^2 \tag{6.a}$$

$$V_2 = A_{21} + A_{22}T \tag{6.b}$$

where $A_{11} = 1.3081\ cm^3/g$, $A_{12} = 1.294\times10^{-3}\ cm^3/gK$, $A_{13} = 1.822\times10^{-6}\ cm^3/gK^2$, $A_{21} = 0.9166\ cm^3/g$ and $A_{22} = 5.8419\times10^{-4}\ cm^3/gK$.

The dodecane concentration dependence of glass transition temperature of polystyrene, Tg, was correlated as in equation (7) [33].

$$Tg = 99.81 - 492.01\ \varphi_1 + 877.33\ \varphi_1^2 \quad (7)$$

The temperature and concentration dependence of the shift factor, a, above glass transition temperature [33] was generalized to the WLF equation as represented in equation (8.a), whereas the shift factor below glass transition temperature was linearly correlated with temperature as in equation (8.b).

$$\log a(T, \varphi_1) = -C_1(T-T_0)/(C_2 + T - T_0) \quad \text{for } T>Tg \quad (8.a)$$

$$\log a(T, \varphi_1) = -C_3\,(T - T_0) \quad \text{for } T<Tg \quad (8.b)$$

where the values of C_1, C_2 and C_3 are 14.8, 48.3 and 0.15, respectively, and the reference temperature, T_0, is the glass transition temperature of each system.

Equilibrium bulk and shear moduli have two limiting values $G_{E,g}$ and $G_{E,r}$, $K_{E,g}$ and $K_{E,r}$ at temperatures well above and well below Tg. The temperature and concentration dependence of $K_{E,r}$ was given by the following Tait expression [32]:

$$K_{E,r}(\phi_1, T) = -V\left(\frac{\partial P}{\partial V}\right)_{T,Eq} = \frac{V(\phi_1, P, T)[P + B(\phi_1, T)]}{CV(\phi_1, 0, T)} \quad (9)$$

$$B(\varphi_1,T) = B_1(\varphi_1)\ \exp\ (-\ B_2(\varphi_1)T) \quad (10.a)$$

$$B_1(\varphi_1) = B_{11} + B_{12}\ \varphi_1 \quad (10.b)$$

$$B_2(\varphi_1) = (B_{21} + B_{22}\ \varphi_1) \times 10^{-3} \quad (10.c)$$

Here, C = 0.0894, the values of B_{11}, B_{12} and B_{21}, B_{22} are 223.7, -96.76 MPa and 3.7801, 2.904℃$^{-1}$ respectively. The limiting values of $K_{E,g}$ and $G_{E,g}$ were determined to be 3.5 and 1 GPa, respectively. The magnitude of $G_{E,r}$ was assumed to be constant (~10^6 MPa) [34], as it is negligibly small compared with that of $K_{E,r}$(~10^9 MPa) in magnitude. Consideration of the moduli at transition between two limiting equilibrium moduli suggested the following models in describing equilibrium moduli.

$$K_E(T, \phi_1) = K_{E,r} + \frac{K_{E,g} - K_{E,r}}{a(T, \phi_1)^{-1/2} + 1} \quad (11.a)$$

$$G_E(T, \phi_1) = G_{E,r} + \frac{G_{E,g} - G_{E,r}}{a(T, \phi_1)^{-1/2} + 1} \quad (11.b)$$

The discrete relaxational shear spectrum, G_i vs. λ_i representing the shear relaxation function was obtained [33] by analyzing the frequency dependent shear modulus experimentally determined.

$$G_\Delta(t, \phi_1) = \sum_{n=0}^{ng} G_i \exp\left(\frac{-t^*}{\lambda_i}\right) \quad (12.a)$$

The bulk modulus, K(t), was determined from the correlation between the bulk modulus, longitudinal bulk modulus, M(t), and shear modulus, G(t), as reported in several literature [34]. The dynamic longitudinal bulk modulus was determined from an acoustic experiment [35-37] by measuring the longitudinal velocity and attenuation coefficient of an ultrasonic wave transmitting through the sample.

$$K_\Delta(t, \phi_1) = \sum_{n=0}^{ng} K_i \exp\left(\frac{-t^*}{\lambda_i}\right) \quad (12.b)$$

The resulting corelation between H_i (G_i or K_i) and λ_i is represented in Fig. 1. The effect of temperature and concentration on the relaxation time was given by a shift function as in equation (5.a).

The temperature dependence of polystyrene/dodecane interaction parameter, χ_1, was functionalized as follows [38]:

$$\chi_1 = 1.7131 - 0.0075\ T \quad (60\ < T < 160℃) \quad (13)$$

The temperature and concentration dependence of diffusion coefficient, D_{12}, [39] was expressed by Vrentas and Duda's free volume model:

$$D_{12} = \frac{D_0\rho_2 V_2 \rho_1}{RT} \exp\left[-\frac{\gamma(w_1 V_1^* + w_2\xi^* V_2^*)}{V_{FH}}\right]\left(\frac{\partial \mu_1}{\partial \rho_1}\right) \quad (14)$$

where

$$\xi = V_1^* M_1 / V_2^* M, \quad (15)$$

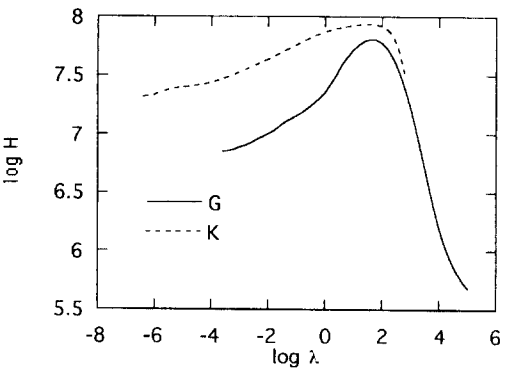

Fig. 1. Shear and bulk relaxation spectra of polystyrene.

$$\frac{V_{FH}}{\gamma} = (K_{11}/\gamma)w_1(K_{21} + T - T_{g1}) + (K_{12}/\gamma)w_2(K_{22} + T - T_{g2}) \quad (16)$$

Here, $V_1^* = 1.071\ cm^3/g$, $V_2^* = 0.85\ cm^3/g$, $K_{12}/\gamma = 5.16\times10^{-4}\ cm^3/gK$, $K_{22} - T_{g2} = -324.7\ K$, $K_{11}/\gamma = 0.001325\ cm^3/gK$, $K_{21} - T_{g1} = -79.03\ cm^3/gK$, $D_0 = 4.6\times10^{-5}\ cm^2/s$, and $\xi = 0.41$.

The concentration and temperature dependence of diffusion coefficient below the glass transition temperature was given by estimating a parameter characterizing the volume contraction attributed to the glass transition. The resulting value of diffusion coefficient below glass transition temperature was $3.16\times10^{-11}\ cm^2/s$ [39].

5.2. Model Predicted Mass Uptake Behavior

Once all material parameters were determined, kinetics of surface concentration, concentration and stress profiles in the polymer films could be predicted by complex mathematical treatment with functionalized material properties. In current study, a system was considered where the polymer was in free contact with the fluid on two opposite sides so that the polymer might swell only in one direction.

The time dependent fractional penetrant mass uptake characterizing the overall transport kinetics is obtained by numerical integration of penetrant concentration profiles within the polymeric system over the entire volume.

$$\frac{M_t}{M_\infty} = \frac{\int\int\int \rho_1 dV}{\rho_{1,eq} V_{eq}} = \frac{1}{L_0}\left(\frac{1}{\phi_{1,eq}} - 1\right)\int_0^{L_0} \phi_1(x,t)\,dx \quad (17)$$

In Fig. 2(a), (b), (c), (d), and (e), the resulting fractional mass uptake behavior was illustrated at 120, 105, 90, 70, and 40℃, respectively. The transport processes were dependent on the system temperatures. At 120 and 105℃ which was above Tg of undiluted polymer, no significant viscoelastic relaxation contribution to the overall transport processes was observed, as the viscoelastic relaxation was relatively fast so that the pure concentration dependent diffusion mechanism might govern the transport processes. Although the transport behavior at 120 and 105℃ seemed like that of Fickian, the value of n was not exactly 0.5 due to the concentration dependence of diffusion coefficient.

The most interesting phenomenon in this mass uptake phenomenon was shown when the system temperatures were 10 to 40℃ below the glass transition temperature of dodecane-free polymer, as the glassy to rubbery transition occurred during transport process at these temperatures.. As the temperature was decreasing from 105 to 70℃, the transport behavior seemed to change from Fickian to Case II, because of the increase in the concentration dependence of diffusion coefficient and the increase in the mechanical relaxation contribution due to the glassy/rubbery transition induced by dodecane plasticization. At these temperatures the concentration profiles possessed relatively sharp fronts at the swelling interface, as the penetrant diffusion rate reduced in the unswollen, glassy region. As the mechanical modulus in the glassy state was also much higher than that in the rubbery state, even a minute swelling strain gave a big stress gradient in the transition interface. This competetive contribution from the concentration gradient and stress gradient deviated resulting mass uptake behavior from Fickian to

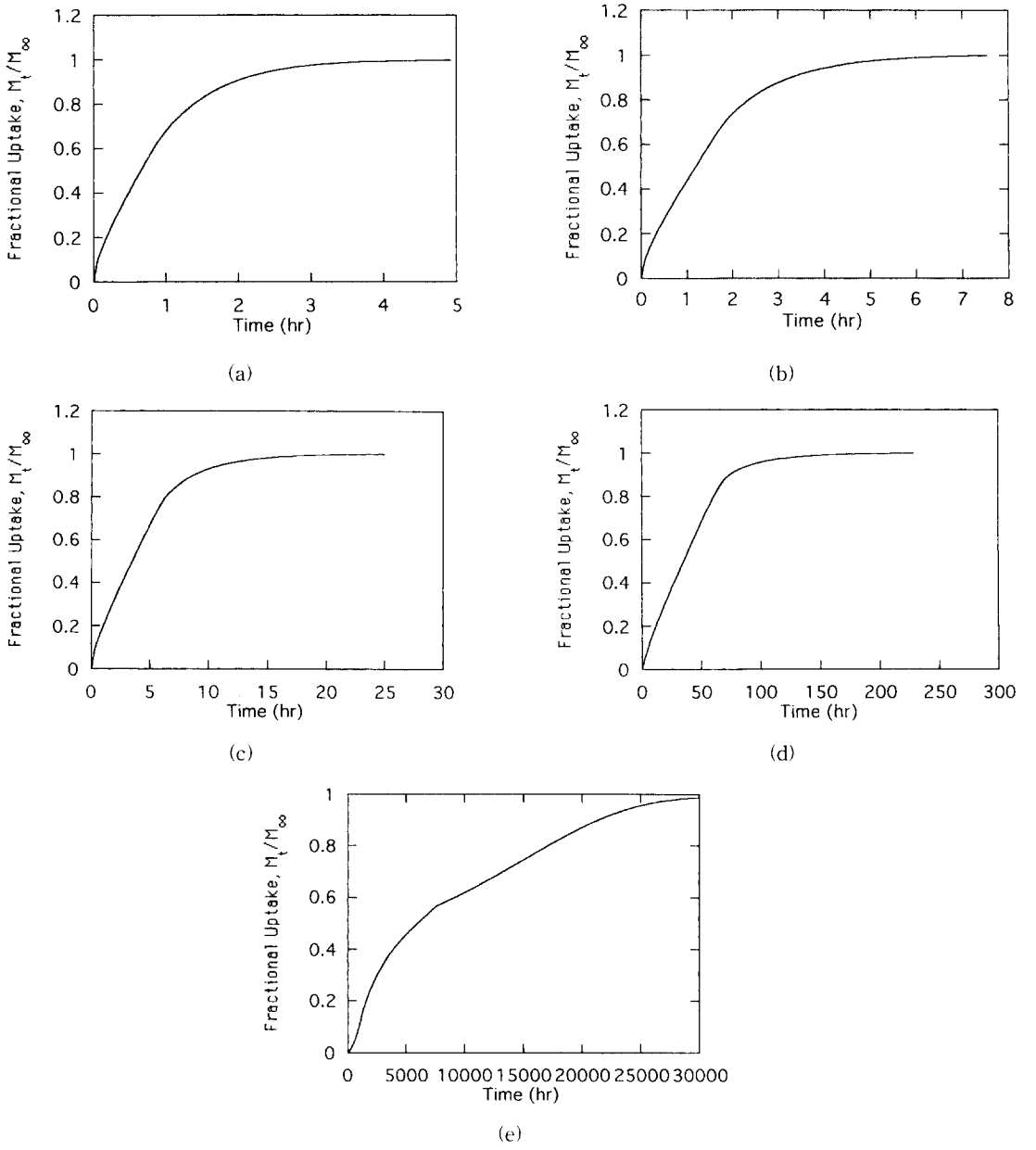

Fig. 2. Fractional dodecane mass uptake determined from the prediction model as a function of diffusion time at various temperatures of 120 (a), 105 (b), 90 (c), 70 (d) and 40℃ (e).

non-Fickian.

We observed more distinct penetrant transport behavior at 40℃ which was well below the glass transition temperature of the polymer system. There was a slight induction period in the initial stage of mass uptake. After an induction period, the mass uptake was accelerated, and then decelerated. Occurrence of this particular transport behavior is explained by the relative importance of the concentration gradient driving force to the stress gradient driving force. In the induction period of the very initial stage of mass uptake,

the penetrant transport was driven by a small concentration gradient and a small stress gradient due to minute penetrant concentration and strain at the polymer/penetrant interface. After a short induction period to attain an appropriate content of penetrant in the polymer/ penetrant interface, there was a period when both the penetrant concentration gradient driving force and the stress gradient driving force were increasing and positively contributing to the penetrant uptake. This period is indicated by the acceleration of mass transport. The decelerating penetrant transport rate starting at the diffusion time around 3000 hr resulted from the negligible stress gradient driving force, even if the chemical potential gradient corresponding to the concentration gradient was still increasing to maximum when the surface penetrant concentration reached the equilibrium concentration. When the surface concentration reached the equilibrium concentration, the mechanical modulus of the material incorporating the equilibrium concentration began to reduce significantly due to the glassy to rubbery state transition. Thus, after equilibrium surface concentration was attained, the stress gradient driving force gave very negative contribution against the concentration gradient driving force, resulting in more deceleration of the transport rate. In this period, even the concentration gradient driving force did not give significant contribution, because the concentration profiles were relatively flat within polymeric system. When this negatively acting stress gradient driving force was negligible in the final stage of the mass uptake, the transport rate increased again at the diffusion time of around 15000 hr as illustrated.

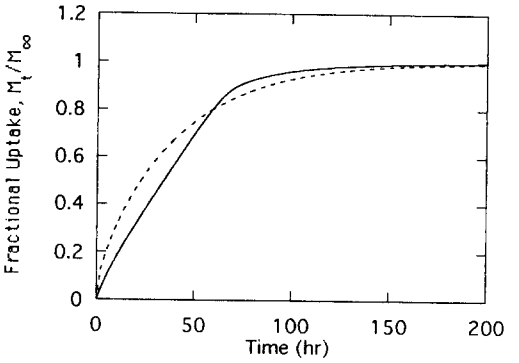

Fig. 3. Fractional solvent mass uptake as a function of diffusion time at 70℃ with constant (dashed curve) and concentration dependent diffusion coefficient (solid curve).

5.3. Effect of Material Properties on Transport Kinetics

In this section we investigated several material parameters that might affect the penetrant transport processes, or, that might increase the stress gradient driving force contribution to the overall penetrant transport behavior.

The primary concern was diffusion coefficient. Fig. 3 shows the time dependent dodecane mass uptake at 70℃ where two functional forms of diffusion coefficient, either constant or concentration dependent, are used. The value of constant diffusion coefficient used in this illustration was 2.51×10^{-10} cm^2/s that was the geometric mean value of the maximum and minimum diffusion coefficients during the penetrant transport. Different functional forms of diffusion coefficient resulted in different penetrant transport processes for

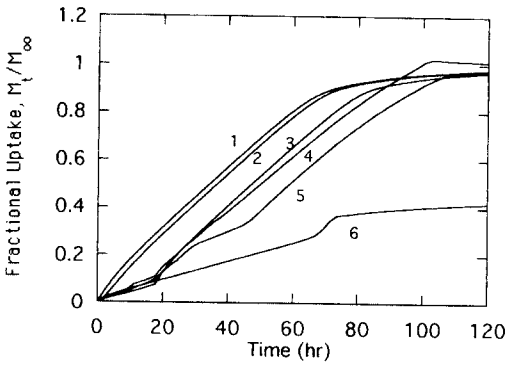

Fig. 4. Effect of viscoelastic relaxation time scale on the transport process at 70℃. Curves from 1 to 6 involve different relaxation time scales: relaxation time is increasing by order of magnitude, 0 (curve 1), 0.7 (curve 2), 1.2 (curve 3), 2 (curve 4), 3 (curve 5), and 4 (curve 6).

same polymer-penetrant systems; constant diffusion coefficient resulted in the transport behavior similar to Fickian diffusion, but concentration dependent diffusion coefficient resulted in the anomalous behavior significantly deviated from the Fickian behavior. It was also of interest to observe the effect of functional description of diffusion coefficient below the glass transition temperature on the overall transport behavior. Throughout the present research, the constant diffusion coefficient, 3.16×10^{-11} cm^2/s, was used to describe the diffusion behavior below the glass transition temperature of the system. The functional description of diffusion coefficient below the glass transition varying from constant to the same concentration dependence as that above the glass transition temperature did not make significant difference to the penetrant mass uptake behavior. It was because the value of actual diffusion coefficient below the glass transition temperature was so small that the concentration dependence of diffusion coefficient might be negligible, even if the logarithmic diffusion coefficient seemed to have considerable concentration dependence. In this analysis, the description of other material properties were kept the same.

The second parameter was the scale of discrete viscoelastic relaxation time, λ_i. Fig. 4 shows the effect of relaxation time on the time dependent mass uptake at 70℃. Increasing the normalized relaxation time scale, $\overline{\lambda}_i$ (= $\lambda_i D_{ev}/L_0$), by order of magnitude from 0 to 4, resulted in a significant change of the transport kinetics, from anomalous to Super Case II through Case II. Under the situation that other material properties were kept constant, increasing relaxation time changed the relative rate between the pure diffusion process and the viscoelastic relaxation process by leading more mechanical relaxation contribution to the transport process. Shift factor decrease due to the penetrant plasticization also should be considered in this relaxation time scale. It should be noted that the penetrant concentration increase during penetrant transport decrease the relaxation time of pure polymer.

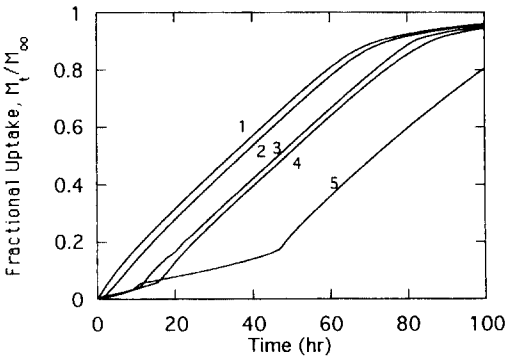

Fig. 5. Effect of viscoelastic relaxation strength on the transport process at 70℃. Curves from 1 to 6 involve different relaxation strength, K_i: $K_i/K_{i0}=1$ (curve 1), 1.5 (curve 2), 3 (curve 3), 4.5 (curve 4), and 6 (curve 5).

The third parameter was the magnitude of discrete viscoelastic relaxation modulus, K_i. Fig. 5 shows effect of viscoelastic relaxation modulus on the transport processe at 70℃. The transportt kinetics changed significantly from Fickian to Non-Fickian as the magnitude of normalized modulus of $\overline{K}_i$ (= K_iV_2/RT) increased. In reality, this factor is not as significant as the other two parameters, because the magnitude of K_i is roughly invariant with the change of polymeric systems.

The overall factor that governs the transport kinetics is temperature [40], as it determines all other material properties of the system of interest. Fig. 6 shows the exponent, n, as a function of temperature for the present system. Above the glass transition temperature of dodecane-free polystyrene, the transport kinetics resembled Fickian. The penetrant diffusive flux was mainly driven by the penetrant concentration gradient starting from the equilibrium swollen free edge. The reason that increasing temperatures led to decreasing values of n, was that the concentration dependence of diffusion coefficient reduced with increasing temperature and concentration. Therefore, the exact Fickian behavior indicated by exponent n = 0.5, is expected at very well above the glass transition temperature where the concentration dependence of diffusion coefficient

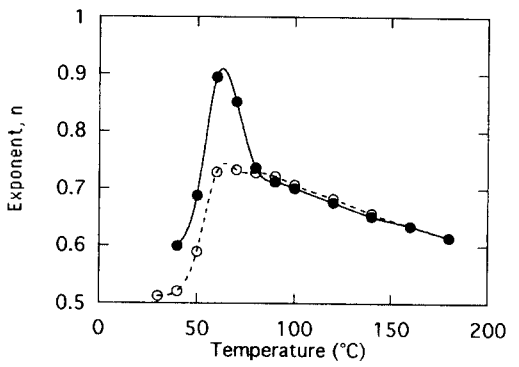

Fig. 6. Exponent, n, as a function of temperature for the transport process (filled circles) driven by both chemical potential gradient and polymer stress relaxation, or for the transport process (open circles) driven by only chemical potential gradient.

is negligible. The viscoelastic relaxation contribution to the transport kinetics began around the glass transition temperature of dodecane-free polystyrene, 100℃, even if its contribution was not significant, yet. From the glass transition temperature of the dodecane-free polystyrene to that of the dodecane-polystyrene system where the glassy/rubbery state transition occurred within the polymeric system during penetrant transport, a discontinuous swelling interface was formed. The polymer stress gradient driving force directed against the penetrant chemical potential gradient driving force retarded the net penetrant transport rate. As a result of it, the transport kinetics was considerably affected by the glassy/rubbery state transition in these temperatures. The viscoelastic relaxation effect was the most significant around the temperatures, 70 to 60℃ for the present system. When the actual temperature is well below the glass transition temperature of the system concerned, the transport kinetics returned to Fickian. Initially, it was possible to have an induction time to achieve the general Fickian sorption.

6. Conclusions

This work overviews experimental observation and theoretical prediction of solvent transport phenomena in polymeric materials. The continuum field theory provided a unified and detailed description of penetrant transport in polymeric systems by incorporating fundamental driving forces: polymer relaxation, thermodynamic mixing and momentum conservation.

The transport behavior numerically predicted founded on the continuum transport framework was illustrated for the dodecane/polystyrene system. Several material properties incorporated in the model were appropriately functionalized. Several types of transport behavior were predicted at varying system temperatures. In general, Fickian characteristics were observed well above and well below the glass transition temperature. Transport nature deviated significantly from Fickian, when the diffusion rate and relaxation rate are on the same scales.

Nomenclature

English letters

a_T : temperature dependent shift factor
B : Tait parameter for equation of state
B : left Cauchy-Green strain tensor
C : universal constant for the Tait equation
C : right Cauchy-Green strain tensor
$C_t(s)$: relative right Cauchy-Green strain tensor
D_a : self diffusion coefficient for component a
D_{eq} : mutual diffusion coefficient at equilibrium concentration
D_{12} : mutual diffusion coefficient
E : almansi strain tensor, **B** - **I**
G_E : elastic shear modulus
G_i : discrete shear relaxation magnitude
G_{∞} : time dependent shear relaxation modulus
I : unit tensor
I : first strain invariant of Cauchy-Green deformation tensor
j_a : diffusion flux for a component a
k : sorption rate constant
K_E : elastic bulk modulus
K_i : discrete bulk relaxation modulus
K_{∞} : time dependent bulk relaxation modulus

L_0 : half-thickness of polymer slab
M_r : molecular weight of repeating unit
M_∞ : equilibrium solvent mass uptake
n : sorption rate exponent
R : gas constant
t : laboratory time scale
t^* : material time scale
T : temperature
T_0 : reference temperature
Tg : glass transition temperature
$\mathbf{T}_a$: partial stress tensor of component a
V_a : specific volume of component a
V_a^* : specific core volume of component a
ω_a : weight fraction of component a

Greek letters

χ_1 : polymer-solvent interaction parameter
φ_a : volume fraction of component a in mixture
λ_i : discrete viscoelastic relaxation time
μ_a : chemical potential per unit mass of a component
ρ_a : component mass density
ξ^* : material time scale

Dimensionless groups

$\overline{D}_{12}$: normalized mutual diffusion coefficient (D_{12}/D_{eq})
$\overline{G}_i$: normalized discrete shear modulus (G_iV_2/RT)
$\overline{K}_i$: normalized discrete bulk modulus (K_iV_2/RT)
$\overline{\lambda}_i$: normalized discrete relaxation time (λ_iD_{eq}/L_0)
$\overline{G}_E$: normalized equilibrium shear modulus (G_EV_2/RT)
$\overline{K}_E$: normalized equilibrium bulk modulus (K_EV_2/RT)

References

1. R. W. Connelly, N. R. McCoy, W. J. Koros, H. B. Hopfenberg, and M. E. Stewart, *J. Appl. Polym. Sci.*, **34**, 703 (1987).
2. J. P. Harmon, S. Lee, and J. C. M. Li, *J. Polym. Sci., Polym. Chem. Ed.*, **25**, 3215 (1987).
3. C. H. M. Jacques and H. B. Hopfenberg, *Polym.. Eng. Sci.*, **14**, 449 (1974).
4. N. L. Thomas and A. H. Windle, *Polymer*, **21**, 613 (1980).
5. N. L. Thomas and A. H. Windle, *Polymer*, **22**, 627 (1981).
6. N. L. Thomas and A. H. Windle, *Polymer*, **23**, 529 (1982).
7. T. Alfrey, Jr., E. F. Gurnee, and W. G. Lloyd, *J. Polym. Sci.*, **C12**, 249 (1961).
8. J. S. Vrentas, C. M. Jarzebski, and J. C. Duda, *AJChE*, **21**, 894 (1975).
9. J. S. Vrentas and J. L. Duda, *J. Polym.. Sci., Polym. Phys. Ed.*, **15**, 441 (1977).
10. J. S. Vrentas, J. L. Duda, and W. J. Huang, *Macromolecules*, **19**, 1718 (1986).
11. P. L. Ritger and N. A. Peppas, *Fuel*, **66**, 815 (1987).
12. H. L. Frisch, T. T. Wang, and T. K. Kwei, *J. Polym. Sci.*, **A2**, 7, 879 (1969).
13. T. T. Wang and T. K. Kwei, *Macromolecules*, **6**, 919 (1973).
14. N. A. Peppas and J. L. Sinclair, *Coll. Polym. Sci.*, **261**, 404 (1983).
15. J. Crank, *J. Polym. Sci.*, **11**, 151 (1953).
16. J. Crank, "The Mathematics of Diffusion", 2nd. Ed., Oxford University Press, NY, 1975.
17. S. R. Lustig and N. A. Peppas, *J. Appl.. Polym. Sci.*, **33**, 533 (1987).
18. J. H. Petropoulos and P. P. Roussis, *J. Membr. Sci.*, **3**, 343 (1978).
19. A. Peterlin, *J. Polym. Sci., Polym. Phys. Ed.*, **17**, 1741 (1979).
20. G. Astarita and G. C. Sarti, *Polym. Eng. Sci.*, **18**, 388 (1978).
21. G. C. Sarti, *Polymer*, **20**, 827 (1979).
22. C. Gostoli and G. C. Sarti, *Polym. Eng. Sci.*, **22**, 1018 (1982).
23. R. W. Cox and D. S. Cohen, *J. Polym. Sci., Polym. Phys. Ed.*, **27**, 589 (1989).
24. M. Kim and P. Neogi, *J. Appl. Polym.. Sci.*, **29**, 731 (1984).
25. C. Tuesdell, "Rational thermodynamics", 2nd Ed., Springer, New York, 1984.
26. B. D. Coleman, and W. Noll, W., *Arch. Rational Mech. Anal.*, **13**, 167 (1963).

27. B. D. Coleman, *Arch. Rational Mech. Anal.*, **17**, 1 (1964).
28. B. D. Coleman, *Arch. Rational Mech. Anal.*, **17**, 230 (1964).
29. R, B. Bird, R, C. Armstrong, and O. Hassager, "Dynamics of polymeric liquids", 2nd Ed., Vol. 1, Wiley, 1987.
30. S. R. Lustig, J. M. Caruthers, and N. A. Peppas, *Chem. Eng. Sci.*, **47**, 3037 (1992).
31. D. Kim, J. M. Caruthers, and N. A. Peppas, *Chem. Eng. Sci.*, **51**, 4827 (1996).
32. D. Kim, N. A. Peppas, and J. M. Caruthers, *J. Polym. Sci., Polym. Phys. Ed.*, **32**, 1593 (1994).
33. D. Kim, J.M. Caruthers, and N.A. Peppas, *Polymer*, **34**, 3638 (1993).
34. J. D. Ferry, "Viscoelastic Properties of Polymers", 3rd Ed., Wiley, New York, 1980.
35. J. Wang, M.S. Thesis, Purdue University, West Lafayette, IN, 1992.
36. L. Piche, F. Massines, G. Lessard, and A. Hamel, Proc. IEEE. Ultrasonic Symposium, 1125, 1987.
37. L. Piche, F. Massines, A. Hamel, and C. Neron, U.S. 4,754,645, 1988.
38. D. Kim, J. M. Caruthers, and N. A. Peppas, *Macromolecules*, **26**, 1841 (1993).
39. D. Kim, J. M. Caruthers, N. A. Peppas, and E. Meerwall, *J. Appl. Polym. Sci.*, **51**, 661 (1994).
40. D. Kim and N. A. Peppas, *KJChE*, **13**, 123 (1996).